Infrared Physics & Technology 52 (2009) 113–118

Contents lists available at ScienceDirect

Infrared Physics & Technology

journal homepage: www.elsevier.com/locate/infrared

Ar^+ ion milling of InSb for manufacturing single electron devices

H. Simchi [a,b,*], M. Raastgoo [a], A. Ranjbar [a], T. Barzekar [a], M. Qasempour [a], M. Daaraei [a], E. Mahmoodzadeh [a], M.H. Saani [a], Sh. Mohammadnejad [b]

[a] Semiconductor Component Industry (SCI), 4 Km of Lashkarak Exp. Way, After minacity four ways, Shahid Langary St., Nobonyad Sq., Pasdaran St., P.O. Box 19575-199, Tehran, Iran
[b] Nao-Optronics Laboratory, Iran Science and Technology University, Heidar Khani St., Resalat St., P.O. Box 16844, Tehran, Iran

ARTICLE INFO

Article history:
Received 14 September 2008
Available online 12 April 2009

PACS:
81.05.Ea
III–V Semiconductors

Keywords:
InSb
Ar^+ milling
Dry etch
Single electron devices

ABSTRACT

Ar^+ ion milling of InSb for manufacturing single electron devices was studied. It is shown that pyramidal structures (porous) are created on the (1 1 1) surface of InSb wafers by anisotropic etching. Also it was shown the axis of the pyramidal structure is a function of the angle of the Ar^+ incident beam and does not depend on the energy of the beam. EDX measurement results show In_xO_y and Sb_xO_y were not created on the surface after milling process. FTIR measurement results show that the surface reflection was decreased and less than 0.3 V flat band voltage was seen in capacitance voltage measurement results. SEM images show that the etching has approximately vertical profile. Therefore the Ar^+ milling technique can be used as a dry etching technique for manufacturing mesa and/or porous structures of InSb. Since the surface is porous and of near-pyramidal morphology, one can simulate the surface by a set of needles each of which is a nanometer-size capacitance (i.e. single electron device). We showed, the threshold voltage of this single electron device is 0.3 V approximately, and therefore it can be used for studying single-electron or Coulomb blockade effects.

© 2009 Elsevier B.V. All rights reserved.

1. Introduction

For devices with sub micrometer dimensions, dry etching is necessary for pattern transfer to maintain vertical profile. In addition to the demands of vertical profile and controllable etch rate, etch-induces damage has to be minimized in order to realize the advantage of these small devices. There are different type of dry etching technology which are, physical sputtering (including ion milling and plasma sputtering), plasma etching (including plasma-assisted chemical reaction) and reactive ion etching (including chemical reaction plus ion bombardment).

Sputter etching in Ar^+ plasma would be an attractive method of in situ surface preparation prior to metal deposition if ion-induced damage of semiconductor surface could be minimized. The Ar^+ sputter etching of GaSb was studied by Polakowska [1].

Her results indicated presence of a damage layer with refractive index $n \approx 5.2$–5.3 and extinction index $k \approx 1.5$. Thus the surface is free from native oxide ($n_{ox} = 1.94$), through the GaSb surface is damaged ($n_{GaSb} = 5.052$) [1].

Ion beam milling is a purely physical technique, with no chemical etching factor. A relatively high energy (500–800 eV) inert ion beam transfer large amount of energy and momentum to the substrate. If the force is strong enough these ions can physically remove material from the sample surface. Usually, the pressure used in ion milling is under the 0.1 millitorr. Since the pressure is low, the mean free path of the particle is long and the ejected sputtered material can cross the reactor vessel and reach opposing walls. When uniform ion beams bombard a sample, it provides an anisotropic profile in pattern transfer.

Atomic layer etching (ALET) of GaAS has been demonstrated by using Cl2/Cl gas and low- energy Ar^+ bombardment. It has been shown that by carefully controlling the reactive species, it is possible to achieve monolayer etching [2,3].

A molecular dynamic study of 50 eV Ar^+ ion bombardment of Si (1 0 0) crystal with a monolayer of adsorbed chlorine has been studied to simulate atomic layer etching of Si. It was shown that, 93% of the silicon removed originated from the topmost silicon layer, the remaining 7% was from the layer underneath [4]. An experimental system and methodology have been developed to realize dry etching of single crystal silicon with monolayer accuracy. They showed control of the ion energy was the most important factor on realizing etching of one monolayer per cycle [5]. Dry etching of SiC in inductively coupled Cl_2/Ar plasma was studied. They showed for the first time, the etch rate of SiC increase by 50% at lower substrate temperatures (−80 °C) than at high substrate temperature (150 °C) [6]. High density plasma etching of RF-sputtered Indium–Zinc-Oxide (IZO) films in Ar, Ar/Cl_2 and Ar/CH_4/H_2 chemistries was studied and it is suggested that, despite its lower etch rate, the Ar/Cl_2 plasma chemistry be privileged over Ar/CH_4/H_2 for IZO etching because it provides a good surface

* Corresponding author. Address: Nao-Optronics Laboratory, Iran Science and Technology University, Heidar Khani St., Resalat St., P.O. Box 16844, Tehran, Iran.
E-mail address: yamahdiadrecny@yahoo.com (H. Simchi).

1350-4495/$ - see front matter © 2009 Elsevier B.V. All rights reserved.
doi:10.1016/j.infrared.2009.04.001

morphology and very moderate surface composition alteration [7].

Others have studied the problems with either ion milling of In-based materials or of conventional dry etching to leads to In-rich surfaces before [23,24]. The ion milling damage in InP and GaAs was studied by Pearton et. al. [23], and reactive ion etch of In-based III–V semiconductors were studied by Pearton et. al., [24].

In this paper, as the authors know for the first time, Ar^+ ion milling of InSb for manufacturing single electron devices was studied. It is shown the pyramidal structures (porous) are created in the (1 1 1) surface of a InSb wafer by anisotropic etching. Also it was shown the axis of the pyramidal structure is a function of the angle of Ar^+ incident beam and dose not depends on the energy of beam. The EDX measurement results show, In_xO_y and Sb_xO_y were not created on the surface after milling process. The FTIR measurement results show the surface reflection was decreased and less than 0.3 V flat band voltage was seen in capacitance voltage measurement results. The SEM images show the etching has vertical profile approximately. Therefore the Ar^+ milling technique can be used as dry etching technique for manufacturing mesa and/or porous structures of InSb. Since the surface is porous in near-pyramidal morphology, one can simulate the surface by a set of needles which each of them is a nanometer-size capacitance (i.e. single electron device). We showed, the threshold voltage of this single electron device is 0.3 V approximately, and therefore it can be used for studying single-electron or Coulomb blockade effect similar to others [22].

2. Preparing the samples

Commercial (1 1 1)A n-type Te-doped (3E14–8E14) InSb wafers were cleaned by CP4A solution [8]. The ions flux and the energy of the systems were set up based on the mentioned values based in the Tables 1 and 2 and Ar^+ milling process has been done.

After ion milling process, the SEM images were taken and, the EXD and FTIR experiment were done on the samples. Then the surface of the samples was covered by a SiO_2 layer by PECVD method [9] and the high frequency CV measurement experiment was done.

3. SEM images

The SEM images are shown in Fig. 2a–d and Fig. 3a and b.

Since the images of different conditions are similar to each other, we show them as a picture. In Fig. 3a the incident angel of Ar^+ is zero and in Fig. 3b is 45°.

4. EDX results

The EXD results are shown in Fig. 4a and b. The Fig. 4a shows the result on the dark areas and Fig. 4b shows the result on white

Table 1
The current of ions and the energy of the system, incident angle, θ, equal to zero.

Experiment no.	1	2	3
Energy	1 KeV	800 eV	650 eV
Ion flux	50 μA/Cm^2	50 μA/Cm^2	50 μA/Cm^2
Process time	2 h	2 h	2 h

Table 2
The current of ions and the energy of the system, incident angel, θ, equal to zero and 45°.

Experiment no.	1	2
Energy	1 KeV, $\theta = 0$	1 KeV, $\theta = 45°$
Ion flux	50 μA/Cm^2	50 μA/Cm^2
Process time	2 h	2 h

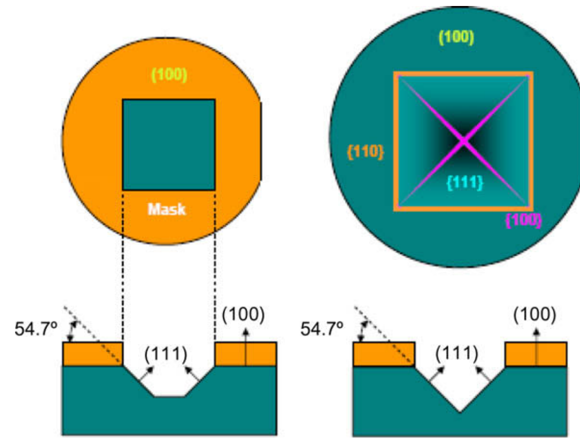

Fig. 1. The typical different planes on III–V wafers.

areas of SEM images. The results show no indium and antimony oxides were created on the surface.

5. FTIR results

The result of the FTIR experiment is shown in Fig. 5a and b before and after dry etches, respectively. As the result show the reflection decreased and the transmission did not change.

6. CV measurement results

After coating the surface by 0.5 μm PECVD SiO_2 [9] a metal layer (Cr(300A)/Au(3500A)) was coated on the surface and capacitance voltage measurement was done. The result of low frequency is shown in Fig. 6a and high frequency in Fig. 6b. Before we have shown [9], on (1 1 1) n-type InSb the flat band voltage is at range 4–5 V. Because we have not indium and antimony oxides on the surface now, the flat band voltage is at the range 0.15–0.2 V. Also since the thickness of oxide is 0.5 μm, and, the capacitor shapes is circle whose radius is 250 μm, the $\varepsilon_{SiO_2}/\varepsilon_0$, 77 K will be equal to:

$$\varepsilon_{SiO_2}/\varepsilon_0 \cong 1.44$$

The ratio is not in fair agreement with our previous data [9] although the deposition process of SiO_2 was same in both of them. Therefore one can conclude the surface morphology of the InSb effects on the property of coated SiO_2 layer.

7. Results and discussion

Anisotropic wet chemical etching remains the most widely used processing technique in silicon technology. During recent years, much effort has been dedicated to the characterization and understanding of the surface morphology during wet chemical etching, both experimentally [10] and theoretically [11]. Realistic Monte Carlo simulation show that the pyramidal hillocks on Si (1 0 0) are the result of local stabilization of distributed apex atoms by (metal) impurities from solution [12].

There is an empirical rule in III–V semiconductor etching that slow etching faces consist of group III atoms, since the group V atoms are electron rich, and hence more reactive [13]. This was the basis for the use of acidic and oxidizing reagents to break the covalent bonds in III–V semiconductors [14,15]. But the main problem of wet etching of InSb is remaining of indium and antimony oxides on the surface after etching process [8]. These oxides cause flat band voltage shifts and non hysteresis-free behavior in capacitance voltage measurement experiment [9]. Therefore people

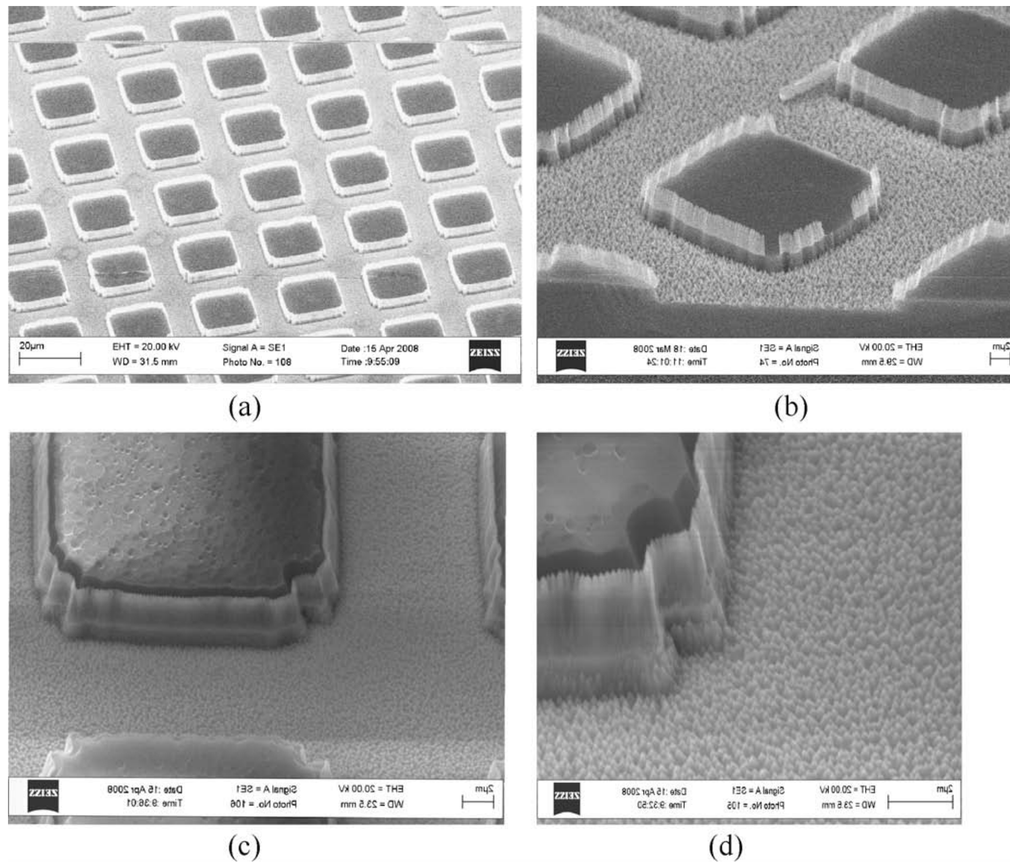

Fig. 2. SEM images after Ar^{+} milling of InSb, ion flux = 50 μA/Cm^2, and energy = 1 KeV, time = 2 h.

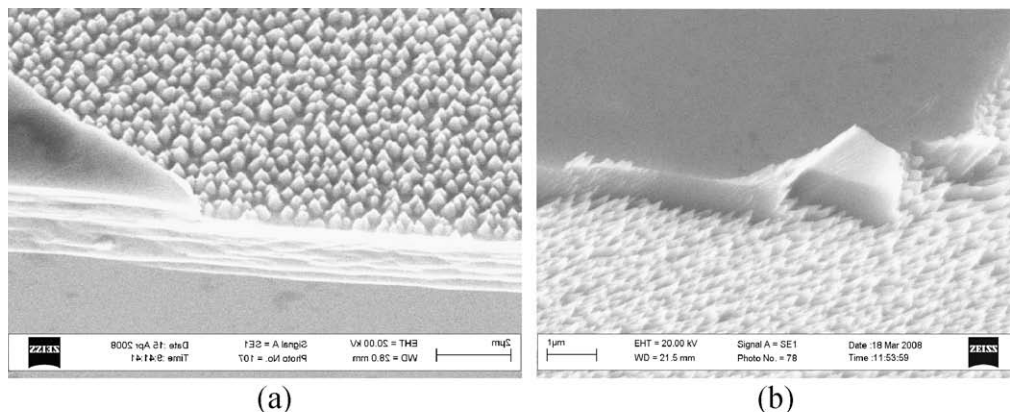

Fig. 3. SEM images at different angle of incident Ar^{+} beam, (a) $\theta = 0$, (b) $\theta = 45°$, ion flux = 50 μA/Cm^2, and energy = 1 KeV, time=2 h.

prefer to use dry etching method instead of wet etching technique for minimizing (or deleting) oxide formation on the surface.

In the other hand, for a compound III–V semiconductor such as InSb for example, indium contributes three electrons ($5s^2$ $5p^1$), and antimony does five electrons ($4s^2$ $4p^3$). Thus a total number is eight valence electrons per basis or four per atom [16]. Due to the different electro negativity, the bonds are partly ionic and thus not purely covalent. Crystal planes are referred to as polar planes, when they do not include equal numbers of group III and group V atoms. These planes will therefore be electrically charged. For a zinc-blende crystal such as InSb for example, the only electrically neutral (non-polar) low-index planes are the (1 1 0) planes. Atoms at the surface have a lower coordination number than the bulk atoms and therefore the surface atomic surrounding is different from the one in the bulk. Each group III atom of the top layer at the (1 1 1)A cation-terminated surface is bonded to the three group V atoms of the layer beneath. If one out of four atoms of group III in the top layer is removed from thee surface, three group V dangling bond orbital will be created. The electrons in the remaining three group III dangling bond orbital are transferred to the three created group V dangling bond orbital. Such reconstruction can be considered in accordance to the group III and it was shown, the (1 1 1)A polar surface, independently of preparation technique, reveal the (2×2) reconstruction only [17,18].

By attention to above descriptions, it can be assumed that, a polar surface of InSb i.e. reconstructed (1 1 1)A polar surface was

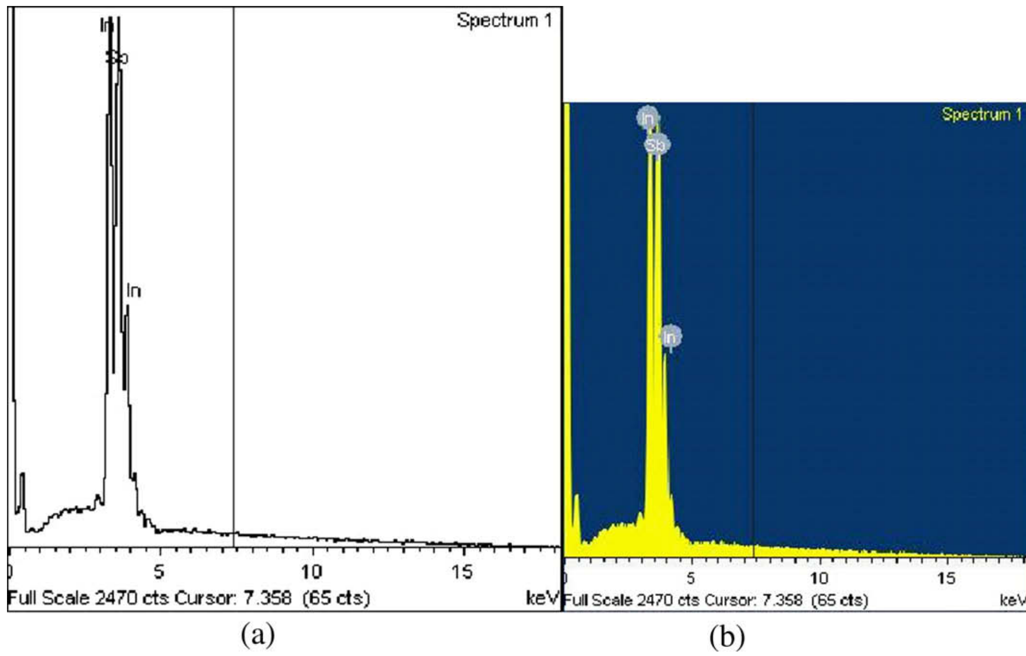

Fig. 4. EDX result at (a) dark and (b) white areas of SEM images.

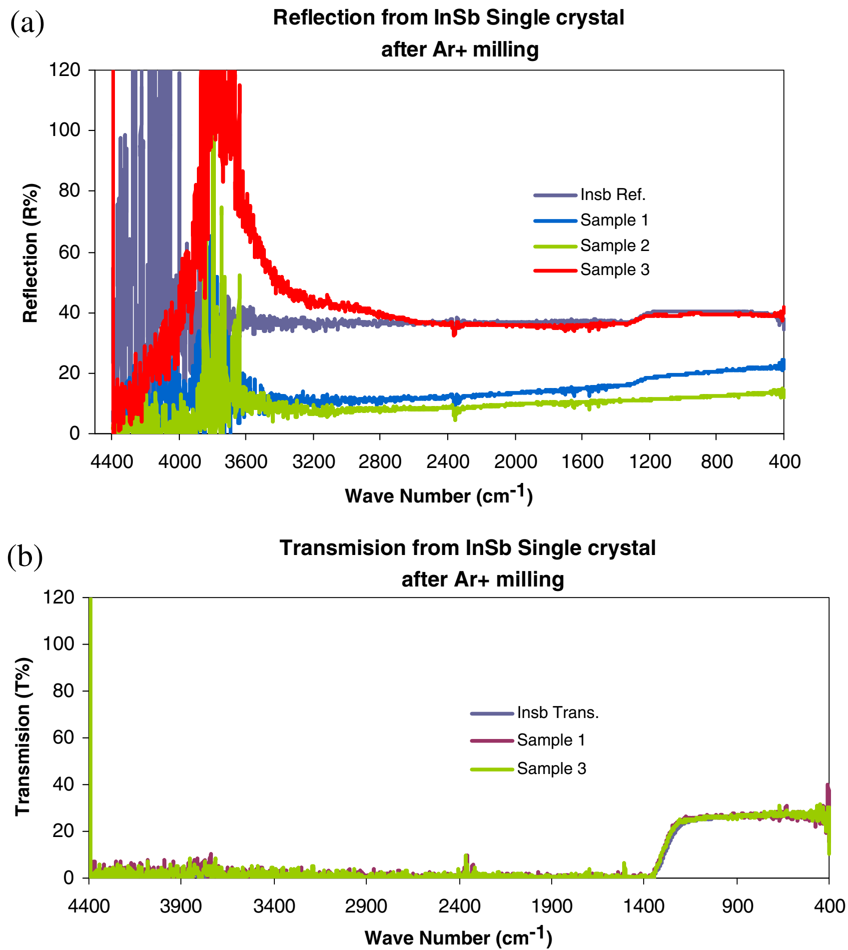

Fig. 5. FITR result (a) reflection and (b) transmission curves, InSb reflection and InSb transmission stand for InSb wafer before Ar^+ milling. The specification of samples was mentioned in table one.

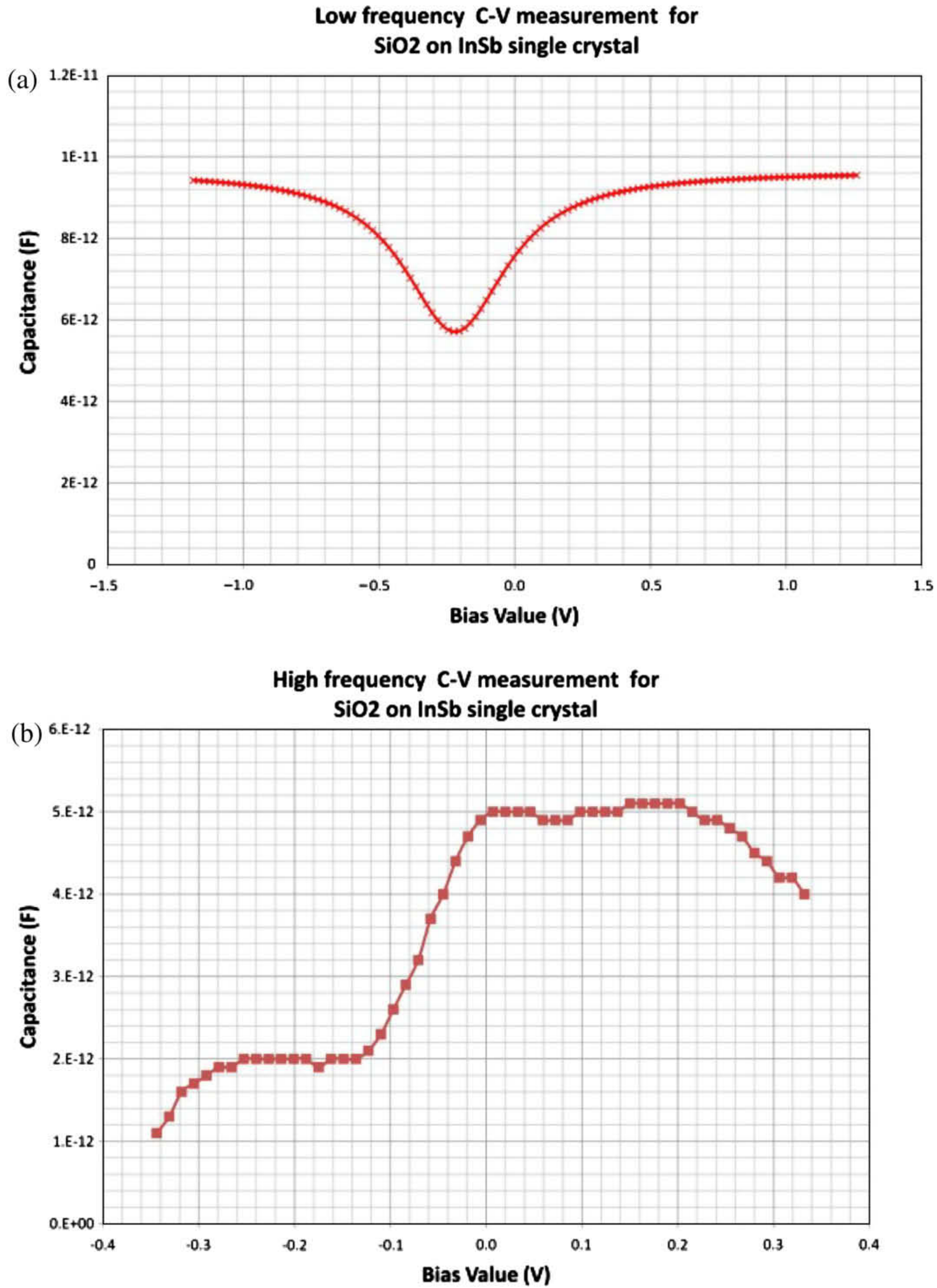

Fig. 6. Capacitance voltage curve (a) low frequency and (b) high frequency.

placed against the flow of Ar^+ at each instant of time. The electric potential which the dipoles produce at point, P, outside the matter is given by [19]:

$$V = \frac{1}{4\pi\varepsilon_0}\int_{S'}\frac{\sigma_b da'}{r} + \frac{1}{4\pi\varepsilon_0}\int_{\tau'}\frac{\rho_b d\tau'}{r} \quad (1)$$

where S' is the surface that bound the volume τ' of the matter. Also σ_b and ρ_b are surface and volume charge distributions, respectively.

Since ion milling is purely physical and requires high energy (500–1000 eV), it can be assumed that the effect of polar surface on Ar^+ ions is negligible.

In the other hand, the surface atom density at {1 1 1} plane is more than {1 0 0} plane and at {1 0 0} plane is more than {1 1 0} plane. Therefore it is expected, as Fig. 1 shows, we have anisotropic etching and therefore a vertical etch profile can be obtained. It is the profile we got and is shown in Fig. 2a–d.

The etch rate, R, is directly proportional to the yield (the number of milled atoms or molecules per incident ion), given by [20]:

$$R = \frac{6.22 sjW}{\rho} \quad \text{(nm/min)} \quad (2)$$

where s is the milling yield, j the ion flux (mA/Cm^2), W the molecular weight of the etched material (g/mol), and, ρ, the density of the material to be etched (g/Cm^3).

The molecular weight of argon is 39.95, the density of InSb is 5.77 gr/Cm^3 at 300 K and in our experiment, the ion flux is 0.05 mA/Cm^2. Therefore the Eq. (2) can be rewritten as:

$$R = 2.23s \quad (\mathrm{nm/min}) \tag{3}$$

We found 0.6–0.8 μm/h etch rate during our experiment for both InSb and AZ9260 photo resist at incident angel equal to zero. Therefore the milling yield is at range 22.30–29.75 nm/min. This approximately small milling rate can be used in nano-technology.

If we assume a pyramidal hillock appear as regular pentahedra composed of four lateral {1 0 0} crystallographic planes lying on the (1 1 1) base plane, the near-pyramidal morphology can be considered as the result of {1 0 0}-terrace bunching due to the relatively fast removal of material from the top and the four near-⟨1 1 0⟩ edges as compared to the slow removal of material from {1 0 0} planes themselves. Because of, we saw near-pyramidal morphology on Ar^+ dry etched InSb as Fig. 3a shows [21].

Fig. 3b shows the result when the Ar^+ beams encountered the surface in 45°. As the figure shows, the direction of the axis of pyramidal is in direction of the incident beam. That is the surface will be porous after dry etching. Because of, we expect the reflection decrease and transmission increase at InSb surface as Fig. 5a and b show.

The result of low frequency CV measurement is shown in Fig. 6a and its high frequency in Fig. 6b. Before we have shown [9], on (1 1 1) n-type InSb the flat band voltage is at range 4–5 V. The EXD results are shown in Fig. 4a and b. The Fig. 4a shows the result on the dark areas and Fig. 4b shows the result on white areas of SEM images. The results show no indium and antimony oxides were created on the surface.

Because we have not indium and antimony oxides on the surface now, the flat band voltage is at the range 0.15–0.2 V. But the ratio $\varepsilon_{SiO_2}/\varepsilon_0$ is not in fair agreement with our previous data [9] although the deposition process of SiO_2 was same in both of them. Therefore one can conclude the surface morphology of the InSb effects on the property of coated SiO_2 layer.

Since the surface is porous in near-pyramidal morphology, one can simulate the surface by a set of needles which each of them is a nanometer-size capacitance. When the voltage increases to more than 0.3 V, as Fig. 6b shows, the current increase suddenly and the device failed. However the idea of single electron electronics is based on the fact that it takes an appreciable amount of energy to transfer a single electron into a structure with a small enough capacitance. The area of near-pyramidal needle is equal to 7.85×10^{-3} μm^2 (diameter 0.1 μm) approximately as Fig. 3 shows. Therefore its associated capacitance is equal to 2×10^{-19} F approximately and it takes a threshold voltage ($V_{threshold} = 1.6 \times 10^{-19}$/C) of 0.8 V. Therefore one can conclude the single electron device (i.e. each needle) transfer the electron to the substrate and the device will be failed if the voltage increases more than 0.8 V theoretically. Of course we estimated the area of near-pyramidal needles and because of, the measured threshold voltage is 0.3 V instead of 0.8 V.

Since we have a single electron device now, one can use it for studying the single-electron or Coulomb blockade effect such as others [22].

8. Conclusion

Commercial (1 1 1)A n-type Te-doped (3E14–8E14) InSb wafers were cleaned by CP4A solution [8]. The ions flux and the energy of the systems were set up based on the mentioned values based in the Tables 1 and 2 and Ar^+ milling process has been done.

Since the surface atom density at {1 1 1} plane is more than {1 0 0} plane and at {1 0 0} plane is more than {1 1 0} plane, it is expected, as Fig. 1 shows, we have anisotropic etching and therefore a vertical etch profile can be obtained. It is the profile we got and is shown in Fig. 2a–d. If we assume a pyramidal hillock appear as regular pentahedra composed of four lateral {1 0 0} crystallographic planes lying on the (1 1 1) base plane, the near-pyramidal morphology can be considered as the result of {1 0 0}-terrace bunching due to the relatively fast removal of material from the top and the four near-⟨1 1 0⟩ edges as compared to the slow removal of material from {1 0 0} planes themselves. Because of, we saw near-pyramidal morphology on Ar^+ dry etched InSb as Fig. 3a shows [21]. Fig. 3b shows the result when the Ar^+ beams encountered the surface in 45°. As the figure shows, the direction of the axis of pyramidal is in direction of the incident beam. That is the surface will be porous after dry etching. Because of, we expect the reflection decrease and transmission increase at InSb surface as Fig. 5a and b show. The EXD results are shown in Fig. 4a and b. The results show no indium and antimony oxides were created on the surface. Because we have not indium and antimony oxides on the surface now, the flat band voltage is at the range 0.15–0.2 V. But the surface is porous in near-pyramidal morphology. Therefore we can simulate the surface by a set of needles which each of them is a nanometer-size capacitance. (i.e. single electron device). We showed, the threshold voltage of this single electron device is 0.3 V approximately, and therefore it can be used for studying single-electron or Coulomb blockade effect similar to others.

References

[1] E. Papis-Polakowska, Electron technology, Int. J. 37/38 (2005/2006).
[2] T. Meguro et al., Appl. Phys. Lett. 56 (1990) 1552.
[3] T. Meguro, Y. Aoyagi, Matter Res. Soc. Symp. Proc. 222 (1991) 121.
[4] Satish D. Athavale, Demetre J. Economou, J. Vac. Sci. Technol. A 13 (3) (1995).
[5] Satish D. Athavale, Demetre J. Economou, J. Vac. Sci. Technol. B 14 (6) (1996).
[6] Liudi Jiang et al., J. Phys. D: Appl. Phys. 37 (13) (2004) 1809–1814.
[7] R. Khanna et al., in: CS MANTECH Conference, Austin, Texas, USA, May 14–17, 2007.
[8] H. Simchi et al., EJP, Appl. Phys. 33 (2006) 1–4.
[9] H. Simchi et al., Infrared Phys. Technol. (September) (2007).
[10] S.-S. Tan et al., J. Microelectromech. Syst. 5 (1996) 66–72.
[11] A.J. Nijdam et al., J. Appl. Phys. 89 (41) (2001) 13–23.
[12] M.A. Gosalvez, R.M. Neminen, New J. Phys. 5 (2003) 100.1–100.28.
[13] I.E. Vermeir et al., J. Electrochem. Soc. 142 (1995) 3227.
[14] P. Bandaru, E. Yablonovitch, J. Electrochem. Soc. 149 (11) (2002) G599–G602.
[15] P. Walker, W.H. Tran, CRC Handbook of Metal Etchants, CRC Press, Boston, MA, 1991. p. 678.
[16] C. Anderson, Doctoral Thesis, TRITA-FYS 3048, Stockholm, Sweden, 1996.
[17] A.U. Mac Rae, Surf. Sci. 4 (1996) 247.
[18] C.B. Duke, Appl. Surf. Sci. 65/66 (1993) 543.
[19] P. Lorrain, D. Corson, Electromagnetic Fields and Waves, Second ed., CBS Publishers, 1986.
[20] David C. Hays, M.S. Thesis, University of Florida, 1999.
[21] S.-S. Tan et al., J. Micromech. Microeng. 4 (1994) 147–155.
[22] F. Raissi et al., IEEE Trans. Electron Dev. (2004) 0018–9383.
[23] S.J. Pearton et al., J. Appl. Phys. 68 (1990) 2760.
[24] S.J. Pearton et al., J. Electrochem. Soc. 137 (1990) 3188.